JOURNAL OF COMPUTATIONAL PHYSICS 25, 104–117 (1977)

A Boundary Condition for Computational Magnetohydrodynamics*,†

IRVIN R. LINDEMUTH

Lawrence Livermore Laboratory, Livermore, California 94550

Received June 17, 1976; revised September 27, 1976

A new "background plasma" method for treating boundaries in Eulerian magnetohydrodynamic computations is presented. Previously unconsidered aspects of plasma confinement by a wall are examined in the formulation of the boundary condition. Innovations include a distinct condition under which a plasma can separate from a wall resulting in an influx of "background plasma," the use of boundary values which are interpreted to be interface values not included in volume integrations, and a condition under which a plasma returns to the wall resulting in a stoppage of the outflux of "background plasma." Excellent agreement is obtained between a Lagrangian computation and an Eulerian computation incorporating the new boundary condition.

INTRODUCTION

Numerical magnetohydrodynamic (MHD), or fluid, computations of plasma behavior are becoming increasingly popular as the available physical models become more sophisticated and the available computers become more powerful. The prime objects of the computations are the various plasma pinch machines at laboratories throughout the world. Initial conditions for the pinch computations are usually a uniform plasma in contact with a confining wall. The physical models for which numerical solutions are attempted will, in general, require the plasma to separate from the wall as an external magnetic field is applied, and consequently a vacuum region is formed between the plasma and the wall. Representation of the vacuum region is a problem which has plagued computational magnetohydrodynamicists since the pioneering calculations of Hain *et al.* [1].

The traditional treatment of the vacuum region, as introduced by Hain *et al.*, has been to create low-density plasma at the wall so that a vacuum never occurs. Most MHD codes with which the author is familiar have used this idea in one form or another. When current flow is perpendicular to the magnetic field, the creation of the low-density plasma is, in principle, legitimate, since, if treated properly, the low-density plasma will move in a manner such that the magnetic field in the low-density plasma is essentially the vacuum field; also, the inertial properties of the low-

† This work performed under the auspices of the U.S. Energy Research and Development Administration under Contract No. W-7405-Eng-48.

ISSN 0021-9991

density plasma can be made unimportant if the density is sufficiently low. One aspect, however, which has not been considered in the literature is the possibility and effect of force-free currents in the low-density plasma created for numerical convenience.

An obvious problem of the "background plasma" approach is the high magnetoacoustic speeds which occur in the background. With explicit numerical methods, particularly, the high magnetoacoustic speeds can severely restrict the time step, as Roberts and Potter [2] have explained in their review of MHD calculations. The problem of high magnetoacoustic speed has been alleviated to some extent in a variety of ways. Implicit numerical methods can, in principle, eliminate it altogether. A second alternative was proposed by Boris [3], who incorporated the displacement current into the MHD equations and then introduced a fictitious speed of light. Some codes use a floor value below which the density is prevented from falling, either by artificially preventing mass flow out of cells or artificially injecting mass into cells which otherwise would drop below the floor value. In the former case, mass which should be in the main plasma is left behind, and in the latter case, the total mass in the problem increases, as it does when plasma is created at the wall. The effect on the main plasma of either case is, of course, dependent on the floor value.

For unbiased pinches driven by strong magnetic fields, the "background plasma" approach has in general proved satisfactory. However, the author has seen calculations from several codes where a numerical wall "hang-up" has occurred with persistent currents flowing in the the low-density, "background plasma" at the wall, resulting in a shielding of the main plasma to some extent from the applied magnetic field. Although there are, of course, experimentally observed cases of wall "hang-up," it is quite suspect to suggest that a "hang-up" due to numerical methods bears any semblance of reality. The success of the method has apparently been limited, also, when applied to reverse-bias pinches in which the initial motion of the plasma is toward, rather than away from, the confining wall. Niblett and Fisher [4] reported that the code of Hain *et al.* encountered difficulties when the reverse bias for theta pinch calculations was above a certain level.

This paper describes the boundary condition used in the computer code ANIMAL—*A New Implicit Magnetohydrodynamic ALgorithm* [5, 6]. The boundary condition is a generalization of the "background plasma" method and leads to solutions which do not exhibit any wall "hang-up." The boundary condition also enables the code to calculate pinches with reverse bias of any magnitude. In addition, the boundary condition enables the code to calculate accurately pinches in which the magnetic field oscillates in a manner such that the plasma alternately separates from the wall and then returns to the wall, clearly a more complex situation than either the standard unbiased pinches or the reverse-bias pinches.

PHYSICAL MODEL

Although the ANIMAL code calculates two-dimensional solutions to MHD model equations which include thermal conduction, resistive diffusion, and atomic physics

and which are applied to cylindrical and toroidal geometries, it is sufficient to consider a one-dimensional, ideal MHD model to illustrate the boundary condition. The model uses a continuity equation, an equation of motion, an internal energy equation, and Faraday's law. The appropriate Eulerian partial differential equations are

$$\frac{\partial \rho}{\partial t} + \frac{\partial}{\partial x}(\rho v) = 0, \tag{1}$$

$$\frac{\partial(\rho v)}{\partial t} + \frac{\partial}{\partial x}(\rho v v) + \frac{\partial p}{\partial x} + \frac{\partial(B^2/2)}{\partial x} = 0, \tag{2}$$

$$\frac{\partial(\rho \epsilon)}{\partial t} + \frac{\partial}{\partial x}(\rho \epsilon v) + p\frac{\partial v}{\partial x} = 0, \tag{3}$$

$$\frac{\partial B}{\partial t} + \frac{\partial}{\partial x}(vB) = 0. \tag{4}$$

In Eqs. (1)–(4) ρ is the mass density, v the fluid velocity, ϵ the specific internal energy, B the magnetic field, and p the material pressure. For completeness, the model requires an equation of state relating p to ρ and ϵ.

For the model Eqs. (1)–(4), the analog of typical pinch calculation conditions is a "slab" of plasma confined between two walls, as illustrated in Fig. 1. Initially the plasma is uniform and in contact with the walls. When the externally generated magnetic field is applied to the plasma, the plasma will separate from the wall if the applied magnetic pressure, $B^2/2$, is larger than the initial plasma pressure p_0, as illustrated in Fig. 2b. Since Eq. (4) is an infinite electrical conductivity approximation, no magnetic flux enters the plasma. However, magnetic flux does enter the void which opens between the plasma and the wall.

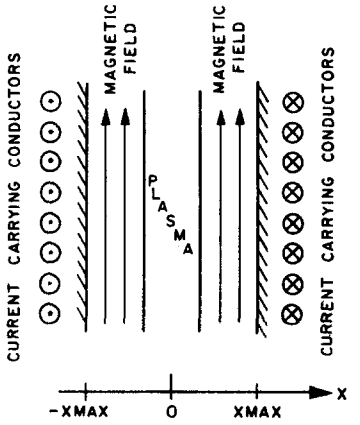

FIG. 1. Simplified plasma pinch geometry.

On the other hand, if the applied magnetic pressure, $B^2/2$, is less than p_0, the net force everywhere on the plasma is identically zero. Therefore, absolutely nothing happens to the plasma, as illustrated in Fig. 2a. For $B^2/2$ less than or equal to p_0, the model equations indicate that the plasma cannot differentiate between wall

confinement, total magnetic confinement, and situations when part of the plasma pressure is supported by the wall and part by the magnetic field. Only the wall can detect the application of the magnetic field because the pressure on it decreases.

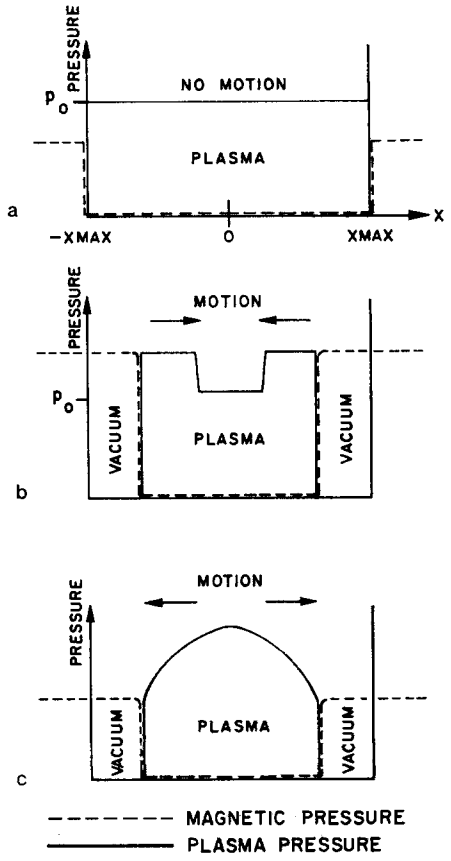

FIG. 2. Distinct cases in a plasma pinch. a. The magnetic pressure is less than the plasma pressure, so the plasma remains stationary. b. The magnetic pressure exceeds the plasma pressure, so the plasma moves away from the confining walls. c. The magnetic pressure drops below the plasma pressure, so the plasma moves toward the walls.

In the plasma there is thus a switch-on effect. For $B^2/2$ less than p_0, nothing happens. When $B^2/2$ exceeds p_0, however, the plasma feels the presence of the magnetic field and moves accordingly.

The switch-on effect is also present in the more complete MHD models which have been incorporated into computer codes such as ANIMAL. The inclusion of resistive diffusion adds a term $\eta(\partial B/\partial x)^2$ to the right-hand side of Eq. (3) and a term $(\partial/\partial x)(\eta(\partial B/\partial x))$ to the right-hand side of Eq. (4); η is the electrical resistivity. When resistive diffusion is present, magnetic field can penetrate into the initially uniform

plasma, causing a net force on interior plasma where the pressure gradient is zero. As the interior plasma moves inward, the plasma pressure at the wall can decrease until it is exceeded by the magnetic pressure gradient at the wall, at which time separation occurs. However, separation can be maintained only if the applied magnetic pressure gradient exceeds the peak plasma pressure.

There is also a switch-off effect indicated by the model Eqs. (1)–(4). When the plasma moves toward the wall, as illustrated in Fig. 2c, the full applied magnetic field is felt by the plasma and the plasma is subsequently decelerated by the field. When the plasma hits the wall, however, the subsequent motion of the plasma is the same as if no magnetic field were present, until the reflection from the wall causes the pressure at the wall to decrease below the value of the applied magnetic pressure, at which time a separation occurs.

Finite Difference Methods

Fundamental to the boundary condition described in this paper is the manner in which the spatial region of interest is divided into finite intervals, or "zones," which determine the points in space at which the dependent variables of Eqs. (1)–(4) are defined. In ANIMAL, the region of interest is divided into JMAX − 2 cells, or zones, and all dependent variables, including velocity, are defined at JMAX points, as illustrated in Fig. 3. The "cell-centered" values such that $2 \leq j \leq \text{JMAX} - 1$ are interpreted physically as being "average" values, so that, for example, the total mass in the problem is equal to the sum of the products of the density and cell volumes. The values of the dependent variables at $j = 1$ and $j = \text{JMAX}$ are interpreted as boundary values; they are considered to be located one-half cell away from the values at $j = 2$ and $j = \text{JMAX} - 1$, respectively, and they are not included in the determination of integral quantities such as mass, thermal energy, etc.

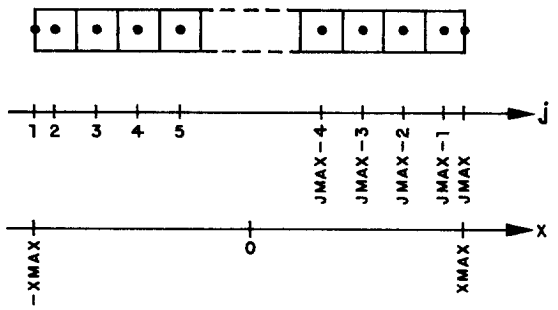

Fig. 3. Zoning used by the ANIMAL code.

To illustrate the boundary condition, it is sufficient to consider approximations to Eq. (1)–(4) which are discretized only in the spatial dimension. The semidiscretized equations are

$$\Delta x \frac{\partial \rho}{\partial t} + (\tilde{\rho}\tilde{v})_+ - (\tilde{\rho}\tilde{v})_- = 0, \tag{5}$$

$$\Delta x \frac{\partial(\rho v)}{\partial t} + \bar{v}_+(\tilde{\rho}\tilde{v})_+ - \bar{v}_-(\tilde{\rho}\tilde{v})_- + F_+ + F_- = 0, \tag{6}$$

$$\Delta x \frac{\partial(\rho\epsilon)}{\partial t} + (\tilde{\rho}\tilde{v}\tilde{\epsilon})_+ - (\tilde{\rho}\tilde{v}\tilde{\epsilon})_- + \bar{p}_+ \delta v_+ + \bar{p}_- \delta v_- = 0, \tag{7}$$

$$\Delta x \frac{\partial B}{\partial t} + \bar{v}_+\bar{B}_+ - \bar{v}_-\bar{B}_- = 0, \tag{8}$$

where

$$F_+ = \delta p_+ + \bar{B}_+\delta B_+, \tag{9}$$

$$F_- = \delta p_- + \bar{B}_-\delta B_-, \tag{10}$$

and where, for convenience, the subscripts $+$ and $-$ are used to replace subscripts $j + \frac{1}{2}$ and $j - \frac{1}{2}$, respectively, and the subscript j has been dropped from all unsubscripted quantities. As usual $\rho_j = \rho(x_j)$, etc., the δ is a difference operator

$$\delta Q_{j+1/2} = (Q_{j+1} - Q_j)/2; \qquad 2 \leq j \leq \text{JMAX} - 2 \tag{11}$$

and the bar indicates an averaging operator

$$\bar{Q}_{j+1/2} = (Q_{j+1} + Q_j)/2; \qquad 2 \leq j \leq \text{JMAX} - 2. \tag{12}$$

Equations (5)–(8) apply for all j such that $2 \leqslant j \leqslant \text{JMAX} - 1$. The tilde ($\sim$) indicates terms which have some arbitrariness. As discussed by Lindemuth [7], Eqs. (5)–(8) conserve total energy and maintain several "subconservation" properties of Eqs. (1)–(4).

The Boundary Condition

In all previous attempts at solving MHD equations numerically, the switch-on and switch-off effects described in a previous paragraph have apparently not been examined closely. For strong field pinches, the main computational difficulty is getting the "vacuum" magnetic flux into the computational domain. For low-field pinches, reverse-bias pinches, and oscillating field pinches, however, the switch-on and switch-off effects must be incorporated in order to properly treat the presence of a wall.

In the following, only the boundary condition at $j = 1$ will be discussed; the boundary condition at $j = \text{JMAX}$ is analogous. The convective fluxes in Eqs. (5)–(8) are written simply as

$$(\tilde{\rho}\tilde{v})_{3/2} = \tilde{\rho}_{3/2}v_1, \tag{13}$$

$$\bar{v}_{3/2}(\tilde{\rho}\tilde{v})_{3/2} = v_1^2\tilde{\rho}_{3/2}, \tag{14}$$

$$(\tilde{\rho}\tilde{v}\tilde{\epsilon})_{3/2} = (\tilde{\rho}\tilde{\epsilon})_{3/2}v_1, \tag{15}$$

$$\bar{B}_{3/2}\bar{v}_{3/2} = B_1v_1, \tag{16}$$

and the compression term of (7) as

$$\bar{p}_{3/2}\delta v_{3/2} = p_2(v_2 - v_1). \tag{17}$$

In Eqs. (13)–(16) it is to be noted that if the boundary velocity v_1 is zero, the values of $\tilde{\rho}_{3/2}$, $(\tilde{\rho}\tilde{\epsilon})_{3/2}$, and B_1 are irrelevant. When v_1 is zero, mass, momentum, thermal energy and magnetic flux are not convected across the $j = 1$ boundary.

The velocity v_1 is initially zero. An examination of the force $F_{3/2}$ is required to determine when the value of v_1 becomes nonzero. $F_{3/2}$ is determined by

$$\begin{aligned} F_{3/2} &= 0, \qquad \text{if } \tfrac{1}{2}(B_1 + B_2)(B_2 - B_1) + p_2 \geqslant 0 \text{ and } v_1 = 0, \\ &= \tfrac{1}{2}(B_1 + B_2)(B_2 - B_1) + p_2 \qquad \text{otherwise.} \end{aligned} \tag{18}$$

If, and only if, $F_{3/2}$ becomes nonzero, v_1 becomes nonzero and is set to

$$v_1 = \tfrac{3}{2}v_2 - \tfrac{1}{2}v_3 \tag{19}$$

for uniform zone size; Eq. (19) is a linear extrapolation.

It should be noted at this time that Eq. (17) guarantees energy conservation when $v_1 = 0$. As shown by Lindemuth [7], the energy flux across the $j = 5/2$ interface due to finite pressure is $\bar{p}_{5/2}\bar{v}_{5/2} = (p_2 + p_3)(v_2 + v_3)/4$; this is most easily shown by using the identity

$$\delta p_+ + \delta p_- = \bar{p}_+ - \bar{p}_- \tag{20}$$

in Eq. (6). With F_- in (6) set to zero, we find that

$$\begin{aligned} \Delta x(\partial/\partial t)(\tfrac{1}{2}\rho v^2) + \cdots &= -v_2\delta p_{5/2} = -v_2(p_3 - p_2)/2 \\ &= -(v_2 + v_3)(p_3 + p_2)/4 + (p_3 + p_2)(v_3 - v_2)/4 + p_2v_2 \\ &= -\bar{v}_{5/2}\bar{p}_{5/2} + \bar{p}_{5/2}\delta v_{5/2} + p_2v_2 \,. \end{aligned} \tag{21}$$

When total energy is summed over the entire domain, the first term on the right-hand side of the last equality in (21) is canceled by an opposite flux, the second term is canceled by the fourth term of Eq. (7), and the last term is canceled by the term in Eq. (17); hence total energy is conserved.

The conditional test indicated by Eq. (18) is a unique feature of the boundary condition reported in this paper. It is sufficient to enable ANIMAL to properly handle the cases depicted in Figs. 2a, 2b. When the applied magnetic pressure is less than the plasma pressure, as in Fig. 2a, $p_2 - B_1^2/2$ is greater than zero, and therefore $F_{3/2}$ is zero. (B_2 is zero since the electrical conductivity is infinite.) When $F_{3/2}$ is zero, absolutely nothing happens. If, however, $p_2 - B_1^2/2$ is less than zero, $F_{3/2}$ becomes nonzero, causing an increase in v_2 and hence v_1, by Eq. (19), is nonzero. There is then a flow of mass, momentum, thermal energy, and magnetic flux into the region of solution as indicated by Eqs. (13)–(16). When v_1 is positive,

$$\tilde{\rho}_{3/2} = \rho_{\mathrm{BG}} \,, \tag{22}$$

$$(\tilde{\rho}\tilde{\epsilon})_{3/2} = \rho_{\mathrm{BG}}\epsilon_{\mathrm{BG}} \,, \tag{23}$$

where the subscript BG indicates "background plasma." The "background plasma" density ρ_{BG} and internal energy ϵ_{BG} are purely arbitrary. By virtue of Eqs. (16) and (19), the vacuum magnetic field is convected into the region of solution by the "back-

ground plasma." Equation (19) ensures that the rate of convection is essentially the $\bar{E} \times \bar{B}$ drift.

For the case of Fig. 2c, v_1 is negative, and $\tilde{\rho}_{3/2}$ and $(\tilde{\rho}\tilde{\epsilon})_{3/2}$ cannot be specified arbitrarily. In this case,

$$\tilde{\rho}_{3/2} = \rho_2 , \tag{24}$$

$$(\tilde{\rho}\tilde{\epsilon})_{3/2} = \rho_2 \epsilon_2 , \tag{25}$$

and the vacuum field and background plasma are convected out of the region of solution. Eventually, however, "real" plasma flows into zone 2 from zone 3, and at this time flow out of the $j = 1$ interface must be stopped. Thus, when v_1 is less than zero, and ρ_2 becomes greater than a "cutoff" density ρ_{co}, v_1 is reset to zero. From then on, $F_{3/2}$ is zero until the test for turning the "background" on is again satisfied.

To be physically precise, the force $F_{3/2}$ should be formulated in terms of the wall pressure as well as the plasma and magnetic pressures. For the case of Fig. 1a, the wall pressure is merely the difference between the applied magnetic pressure and the plasma pressure. Hence, the pressure jump across the plasma–wall interface exactly cancels the jump in magnetic pressure. On the other hand, for the cases of Figs. 1b, 1c, the wall pressure is zero. Equation (18) effectively takes into account the wall pressure under these circumstances.

The test indicated in Eq. (18) is actually a test for separation from the wall and the resetting of v_1 to zero when ρ_2 exceeds ρ_{co} is actually a test for return of the "real" plasma to the wall. Hence, in the ANIMAL code, there are clearly defined conditions of interaction with the wall; when v_1 is zero, the plasma is in contact, and when v_1 is nonzero a "vacuum" region separates the plasma from the wall.

The treatment of the boundary as outlined above is also applicable to the case of finite resistivity. The test indicated in Eq. (18) is again performed, but with finite resistivity, B_2 is no longer zero. When the applied magnetic field is oscillatory, such as in the computation of the preionization phase of a pinch discharge, the plasma can alternately separate and return to the wall during each half cycle of the discharge. The boundary treatment generalizes in a straightforward manner to curvilinear coordinate systems. It is also applicable to two-dimensional computations. In the ANIMAL code, the boundary condition has been used for several different classes of two-dimensional axisymmetric calculations in which only an azimuthal magnetic field was present. In the two-dimensional case there can simultaneously be some boundary cells where the "background plasma" is "on" and others where it is "off." It appears that the boundary treatment can be readily generalized to multicomponent magnetic fields if the boundary is a flux surface, but it is unclear whether or not any fictitious force-free currents will occur in the "background plasma."

It is to be remembered that the zoning as illustrated in Fig. 3 plays an important part in the boundary condition and its interpretation. It is unclear just how one would implement the switch-on and switch-off effects for any other zoning choice or in cases where the dependent variables are not all defined at the same mesh point. Other boundary conditions, such as axis of symmetry or plane of symmetry, can be implemented in a straightforward manner for the zoning of Fig. 3.

Prior to the incorporation of the boundary treatment described here, several fictitious numerical effects were observed in calculations performed with predecessors to the current ANIMAL code and the author has also observed similar effects in calculations performed with other codes. In the treatment of a case analogous to that depicted in Fig. 2a, an oscillatory motion was observed to occur. This motion was due to an improper treatment of the force $F_{3/2}$ in which effectively the pressure gradient at the wall was taken to be zero rather than exactly equal and opposite to the magnetic pressure gradient; hence, the plasma would move away from the wall to establish the required pressure gradient, overshoot the equilibrium value, and oscillate. The same improper treatment also caused fictitious reflected waves from the wall after a plasma returned to the wall after separation.

A variety of other ways was tried to introduce the magnetic flux into the computational domain prior to the identification of boundary values as interface values which determine flow rates into the domain. One approach was to locate boundary values a full cell width from the first interior point and interpret the boundary values as averages over a half-cell. Hence, the magnetic field penetration is always at least one half-cell in length. Allowing the half-cell penetration obviously led to the fictitious oscillations discussed above. In addition, this approach, depending on implementation, led to the "wall hang-up" indicated in the Introduction, since ohmic heating of the boundary half-cell increased its conductivity and convection from the boundary half-cell to the first interior cell did not reduce sufficiently the magnetic field gradient between the two cells. A similar "wall hang-up" would occur in the ANIMAL code if the convection indicated by Eqs. (16) and (19) were not permitted to occur, since the only way magnetic flux could enter the computational domain would be by resistive diffusion whose rate decreases as the plasma ohmically heats. The use of an artificially high resistivity was not satisfactory.

All approaches prior to the one reported here led to very unsatisfactory results when applied to reverse-bias pinches and pinches in which the applied magnetic field was slowly rising. In these instances, a significant amount of time occurs before the condition for turning "on" the background occurs. The test of Eq. (18) assures that no convective processes occur at the boundary until the plasma should actually separate; hence, the time delays prior to separation are handled naturally. In the next section, the boundary condition reported here is applied to a one-dimensional situation in which the magnetic field at one boundary is slowly rising and weak, leading to relatively little separation, and in which the magnetic field is oscillatory, so that a reverse-bias pinch occurs on the second half-cycle.

A Test Problem

To test the boundary condition described above, and, of course, to help test the entire ANIMAL code, we have run a one-dimensional test problem on the Eulerian code ANIMAL and the Lagrangian code HEMPMHD [8]. The physical situation is shown in Fig. 4. The coaxial tube is assumed infinite so that a one-dimensional cal-

culation is sufficient. Initial conditions for the calculation are a uniform deuterium plasma with density $\rho_0 = 3 \times 10^{-4}$ kg/m^3 and temperature $T_0 = 3$ eV. The applied current is sinusoidal with amplitude 450 kA and a period of 20 microseconds. The calculations are followed for 15 microseconds. A fully ionized equation of state is used to describe the plasma, and the physical model used includes thermal conduction and resistive diffusion. The confining insulators are treated as thermal as well as electrical insulators, so no heat is lost from the plasma to the insulators by thermal conduction. For the Eulerian calculation, the region of solution is divided into 45 equally sized zones; for the Lagrangian calculation 38 zones are used. Artificial viscosities similar to the artificial viscosity of von Neumann and Richtmyer [9] are used in both calculations.

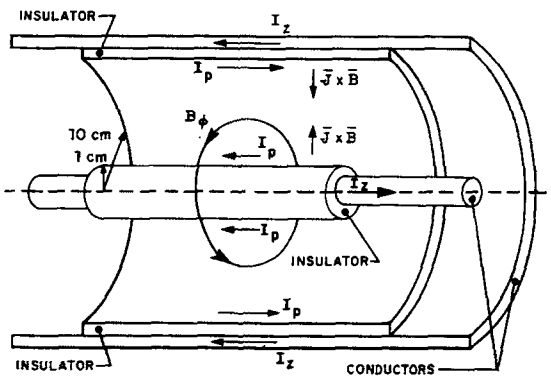

FIG. 4. Geometry for a one-dimensional test problem.

HEMPMHD is a code which incorporates strength-of-materials into its physical model. It therefore can calculate situations in which material spall occurs. Under spall conditions, of course, a continuous piece of material can separate into two distinct pieces. Because HEMPMHD can handle spall, it quite naturally handles separation of a plasma from a confining wall. In a sense, the test of Eq. (18) is modeled after the test for spall used in HEMPMHD.

Figure 5 plots the position of the Lagrangian interfaces versus time for the HEMPMHD calculation. The positions of the innermost and outermost interfaces are of particular interest. The innermost interface does not begin to move until the magnetic field has reached a sufficiently high value; because of resistive diffusion, the interfaces interior to the innermost interface begin to move before the innermost one. The applied current, and hence the applied field, passes its peak at 5 microseconds and the plasma begins to expand toward the center of the coax shortly thereafter. Eventually the innermost interface returns to the confining insulator and remains there as the applied current passes through zero and begins to increase with negative polarity. When the current reaches a sufficiently high value, the innermost interface again moves away from the insulator.

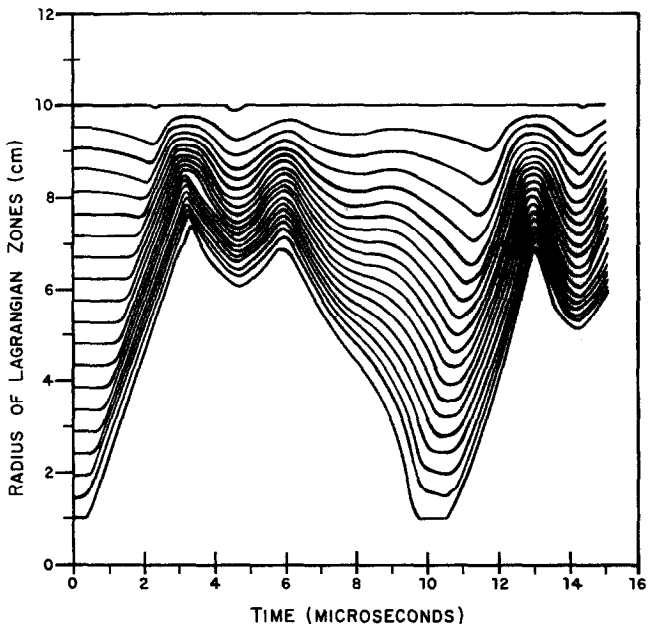

FIG. 5. Position of Lagrangian zone interfaces as a function of time.

TABLE I

Comparison of Separation and Return Times for the Test Problem

	Inner wall	
	HEMPMHD	ANIMAL
Separation	0.3–0.4	0.29
Return	9.6–9.7	9.41
Separation	10.4–10.5	10.57
	Outer wall	
	HEMPMHD	ANIMAL
Separation	2.1–2.2	2.13
Return	2.3–2.4	2.44
Separation	4.2–4.3	4.32
Return	4.9–5.0	4.73
Separation	$\gtrsim$14.2	14.19
Return	$\lesssim$14.4	14.40

Note: All times are in microseconds.

The outermost interface of the HEMPMHD calculation moves away from and then returns to the outer insulator three times, although the first and third times are just barely perceptible in Fig. 5. In each case, the interface moves only slightly before the inverse pinch from the inner insulator overwhelms the z-pinch from the outer region. The second and third separation of the outermost interface occur only because the pressure at the outer insulator can decrease below its equilibrium value when the outward moving compression waves reflect from the outer insulator.

Table I compares the separation and return times for the HEMPMHD and ANIMAL calculations; for the HEMPMHD calculation, data were available only at 0.1 microsecond intervals. Figure 6 compares the increase in thermal energy of the plasma for the two calculations; the maximum difference is less than 10%. For the "background plasma" used in the ANIMAL calculation, ρ_{BG} was 10^{-5} kg/m^3 and T_{BG} was 3 eV. The "cutoff" density ρ_{CO} was 3×10^{-5} kg/m^3. In ANIMAL, thermal conduction, ohmic heating (but not resistive diffusion), and shock heating are turned "off" when the density drops below ρ_{CO} ; the effect of doing so is negligible.

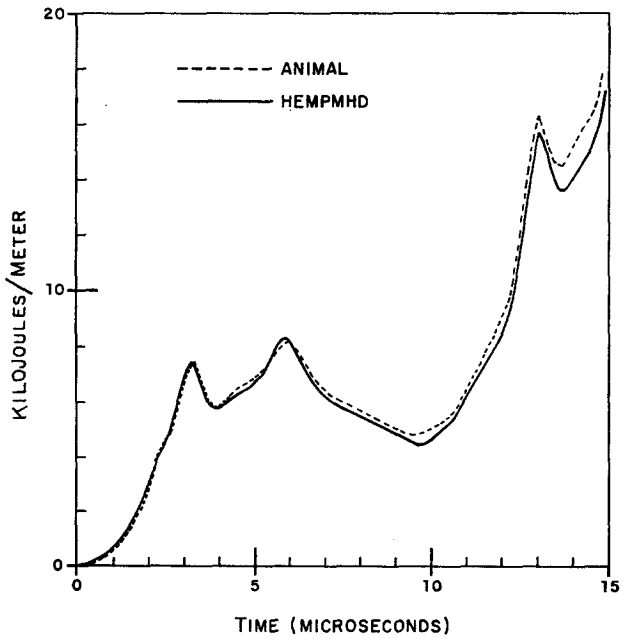

FIG. 6. Increase in total thermal energy for the one-dimensional computations.

Considering the fundamental differences between the Lagrangian and Eulerian formulations, the agreement shown in Table I and Fig. 6 must be considered quite remarkable. Figure 6 shows that at times the spatial resolution of the HEMPMHD calculation is about three times greater than that in the ANIMAL calculation.

Figure 6 also shows that the outer plasma actually moved inward less than the size of an ANIMAL zone before returning to the wall. Because ANIMAL uses alternating-direction implicit finite difference methods [6], its time step size was not limited by the "Courant condition" of the "background plasma" and, in general, the ANIMAL time step was larger than the time step used in the HEMPMHD calculation.

Summary and Concluding Remarks

In the previous paragraphs, a new boundary condition for Eulerian computational magnetohydrodynamics has been presented. The boundary condition incorporates physical aspects which have heretofore been unconsidered. The agreement between the HEMPMHD calculation and the ANIMAL calculation must be interpreted as verifying the accuracy of the boundary conditions and numerical methods of both codes.

The test problem described above has also been run on other codes, several Lagrangian and one Eulerian, which are available at this Laboratory. In general, the agreement was much less than that shown in Fig. 6. The other codes do not have clearly defined separation and return times, and much of the disagreement between the codes can be traced to a failure to properly treat the switch-on and switch-off effects described above. It is clear that to perform accurate MHD calculations, the effect of a confining wall on a plasma must be considered carefully.

Acknowledgment

The author would like to acknowledge the contributions of Dr. Rollin C. Harding, who performed the HEMPMHD calculations and who participated in many valuable discussions.

References

1. K. Hain, G. Hain, K. V. Roberts, S. J. Roberts, and W. Koppendorfer, *Z. Naturforsch. A* **15** (1960), 1039.
2. K. V. Roberts and D. E. Potter, Magnetohydrodynamic calculations, *in* "Methods in Computational Physics" (B. Alder, S. Fernbach, and M. Rotenberg, Eds.), Vol. 9, p. 339, Academic Press, New York, 1970.
3. J. P. Boris, "A Physically Motivated Solution of the Alfuen Problem," Naval Research Laboratory Report 2167 (1970).
4. G. B. F. Niblett and D. L. Fisher, "Numerical Calculations on Reversed Field Heating in the Thetatron," Culham Laboratory Report CLM-R 19 (1962).
5. I. R. Lindemuth, The ANIMAL code, *in* "Proceedings of the Annual Meeting on Theoretical Aspects of Controlled Thermonuclear Research," Roslyn, Va., 1975.
6. I. R. Lindemuth, Numerical methods in the ANIMAL code, *in* "Proceedings of the Seventh Conference on Numerical Simulation of Plasmas," New York, 1975.

7. I. R. LINDEMUTH, *J. Computational Phys.* **18** (1975), 119; Erratum, *J. Computational Phys.* **19** (1976), 338.
8. M. L. WILKINS, "Magnetohydrodynamics of Hemp," Lawrence Livermore Laboratory Report UCRL-51715 (March 1975).
9. J. VON NEUMANN AND R. D. RICHTMYER, *J. Appl. Phys.* **21** (1950), 232.